How Things Get Stuck: Kinetics, Elastohydrodynamics, and Soft Adhesion

Madhav Mani,[1,*] Arvind Gopinath,[2] and L. Mahadevan[1,3,†]

[1]School of Engineering and Applied Sciences, Harvard University, Cambridge, Massachusetts 02138, USA
[2]Martin Fisher School of Physics, Brandeis University, Waltham, Massachusetts 02453, USA
[3]Department of Physics, Harvard University, Cambridge, Massachusetts 02138, USA

(Received 13 December 2011; revised manuscript received 7 February 2012; published 30 May 2012)

We consider the sticking of a fluid-immersed colloidal particle with a substrate coated by polymeric tethers, a model for soft, wet adhesion in many natural and artificial systems. Our theory accounts for the kinetics of binding, the elasticity of the tethers, and the hydrodynamics of fluid drainage between the colloid and the substrate, characterized by three dimensionless parameters: the ratio of the viscous drainage time to the kinetics of binding, the ratio of elastic to thermal energies, and the size of the particle relative to the height of the polymer brush. For typical experimental parameters and discrete families of tethers, we find that adhesion proceeds via punctuated steps, where rapid transitions to increasingly bound states are separated by slow aging transients, consistent with recent observations. Our results also suggest that the bound particle is susceptible to fluctuation-driven instabilities parallel to the substrate.

DOI: 10.1103/PhysRevLett.108.226104 PACS numbers: 68.35.Np, 81.40.Pq, 87.17.Rt

The dynamics of interfacial attachment in a fluid medium, mediated by specific adhesive bonds, is of interest and applicability to several physical and biological systems. Although details regarding the microscopic structure of tethers, distribution of attachment sites, and geometry of the substrates do vary greatly, the essential physics involved is common to various phenomena including the coagulation of subunits in biochemical processes [1], binding using DNA covered nanoparticles [2], aging of a stuck colloid [3], tethering and adhesion of cells [4–8], and the capture efficiency of immersed, sticky surfaces [9]. In these scenarios, substrates come into close proximity, allowing the longest polymeric tethers to provide the initial attachment between substrates. This initial attachment draws the two substrates closer, draining the intervening fluid out and allowing shorter polymeric tethers to themselves provide further attachment. Here we explore this generic attachment process as a function of the basic geometric, structural, and kinetic parameters governing the process.

A minimal model of the phenomena may be idealized in terms of a fluid-immersed spherical particle of radius a that can stick to a flat, rigid substrate grafted with adherent elastic binders, illustrated in Fig. 1(a). The fluid is assumed to have a viscosity μ, density ρ, and temperature θ, with the particle at a distance $[a + h_0(t)]$ from the rigid substrate, as shown in Fig. 1(b). The adherent binders are idealized as polymers with one end attached to the substrate and the other capped by a sticky head of radius a_b. We model each binder as a linear Hookean spring of stiffness $\mathcal{K}_s$ and mean rest length ℓ [10,11]. When subject to thermal fluctuations, the binder heads may eventually contact the particle and stick (here we assume that the reaction is diffusion limited), exerting an elastic force on the particle. If binding events are rare and the mean rest lengths of tethers are well spaced, then the particle may move towards the substrate in a stepwise manner, where long intervals with relatively little motion are punctuated by short busts of transitions to more bound states closer to the substrate; indeed, this phenomenology of punctuated aging is suggested by recent experiments [3].

Owing to the large aspect ratio of the gap between the colloid and the substrate, the viscous drag on the sphere is dominated by lubrication forces and is greater than the viscous drag on the adhesive molecule provided $a/h_0 \sim 10^2 \gg 1$ and $a/a_b \sim 10^4 \gg 1$, respectively, as suggested by using typical values from the cited literature. Additionally, this disparity in sizes allows us to neglect the thermal agitation of the particle while retaining the fluctuations in the binder lengths. In the limit where the areal density of bonds, n_0, is low (typical values being $n_0\ell^2 \sim 10^{-9} \ll 1$), the attached binders do not impede the flow of fluid [12–14].

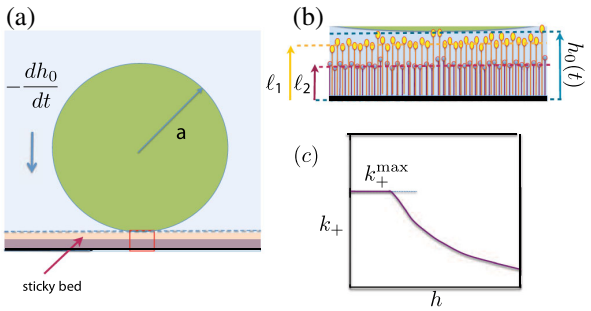

FIG. 1 (color online). (a),(b) Schematic of the system: The center of the particle of radius a lies a distance $a + h_0(t)$ above a substrate. The close-up on the right shows a two-family system, with the rest lengths ℓ_1 and ℓ_2. (c) The binding affinity of a tether, k_+, follows from a Kramer's analysis, saturating when binding events are very likely.

Two additional simplifications allow us to focus on the dynamics normal to the substrate and ignore tangential displacements of the settling sphere. First, we neglect the effect of the shear flow on the mean rest length of the adhesive bonds. Second, we neglect the shearing effect of the mean flow on the binders, thus causing them to bind at an angle to the vertical. This is reasonable provided the torque due to thermal fluctuations dominates the torque on the binder due to the streaming flow. For the shearing flow to have negligible effect on the statistical properties of the bonds, we require $\dot{\gamma}\mu\ell/\kappa \ll 1$ with κ being the characteristic stiffness (a mean field value) of the bonds and $\dot{\gamma}$ being a mean shear rate. Here we assume that the rest length of the tethers is not modified by the flow and, vice versa, that the flow is not modified by the tethers.

Since the motion of the particle towards the substrate drives the fluid out of the intervening gap, the effect of inertia is quantified via the Reynolds number based on the gap size $\mathrm{Re}_{h_0} \equiv \mu(dh_0/dt)(h_0/a)^2 a/\rho \ll 1$. The effect of inertia at the colloid scale $\mathrm{Re} \equiv \mu(dh_0/dt)a/\rho$ is also typically less than unity. For a neutrally buoyant colloidal particle at height

$$h(t) = h_0(t) + a(1 - \sqrt{1 - r^2/a^2}) \tag{1}$$

(r being the radial coordinate) above a substrate that is decorated with Hookean tethers (spring constant K_s) parametrized by their rest length ℓ and number density $n(\ell, t)$, the equation of motion is

$$\frac{6\pi\mu a^2}{h_0}\frac{dh_0}{dt} + 2\pi\mathcal{K}_s\int_\ell d\ell\int_0^a n(r,\ell,t)(h-\ell)rdr = 0. \tag{2}$$

Here the first term in Eq. (2) is the leading order force on the sphere that models the increasing difficulty in draining fluid out of the gap as $h_0 \to 0$ [15], while the second term characterizes the elastic forces on the colloid due to the bound tethers [10,11]. In many biological systems, the distribution of lengths of the tethers is bimodal [11], and so here we study a two-family system of binders for which

$$n(\ell, t) = n_1(t)\delta(\ell - \ell_1) + n_2(t)\delta(\ell - \ell_2), \tag{3}$$

$n_i(t)$ being the areal density of bound bonds of the ith family attached at a height h at time t and $\delta(s)$ is the Dirac delta function. To close Eqs. (1)–(3), we need to specify equations for the binder dynamics. Assuming first-order kinetics for the attachment and detachment process [10,11,16], we write

$$\frac{dn_i}{dt} = k_{\mathrm{on}}(n_{i,0} - n_i) - k_{\mathrm{off}}n_i, \tag{4}$$

where $n_{i,0}$ $(i = 1, 2)$ is the total area density (attached plus detached) of bonds, k_{on} is the attachment rate, and k_{off} is the detachment rate. Given some initial conditions, Eqs. (1)–(5) constitute a set of coupled, nonlinear equations for the height h as a function of n_1 and n_2.

Since the particle is being drawn closer to the substrate rather than being pulled away [11,17], we choose the off rate to be a constant and explore the consequences of a displacement dependent attachment rate. Provided the settling rate is slow, one may assume that binders attach at a rate that depends solely on the distance the heads have to traverse in order to stick to the particle. In this limit, k_{on} depends on the extension $h(t) - \ell$. By adopting a Kramers-style argument [16,18], in the limit of large extension $h \gg \ell + (2k_B\theta/\mathcal{K}_s)^{1/2}$ the asymptotic approximation to the mean first passage time and thus k_{on} yields (Supplemental Material, Sect. I [19])

$$k_{\mathrm{on}} \approx D_b\sqrt{2}(h-\ell)\left(\frac{\mathcal{K}_s}{k_B\theta}\right)^{3/2} e^{-(\mathcal{K}_s/2k_B\theta)(h-\ell)^2}, \tag{5}$$

D_b being the diffusion constant of the binder head. For small extensions, the asymptotic expression (5) is not valid. We note that the maximum value $k_{\mathrm{on}}^{\max}$ is attained at $h = \ell + (k_B\theta/\mathcal{K}_s)^{1/2}$. To obtain a tractable, continuous expression, we set $k_{\mathrm{on}} = k_{\mathrm{on}}^{\max}$ for $h \le \ell + (k_B\theta/\mathcal{K}_s)^{1/2}$.

Typical values for parameters appearing in Eqs. (1)–(5) are $a \approx 10^{-6}$ m, $\mu \approx 10^{-2}$ Pa s, $n_0 \approx (10^7$–$10^9)$ m^{-2}, $a_b \approx 10^{-10}$ m, $\ell \approx 10^{-8}$ m, and $\mathcal{K}_s \approx (0.01$–$10) \times 10^{-3}$ N m^{-1}. To make sense of these values, we introduce the dimensionless variables $H \equiv h/\ell_1$, $R \equiv r/a$, $T \equiv tk_{\mathrm{on}}^{\max}$, $\mathcal{L}_i \equiv \ell_i/\ell_1$, and $N_i \equiv n_i/n_{i,0}$. Then, Eqs. (1)–(5) can be written as the following dimensionless versions:

$$\frac{\alpha}{H_0}\frac{dH_0}{dT} = \int_0^1 [N_1(1-H) + N_2(\mathcal{L}_2 - H)]RdR, \tag{6}$$

$$H(R,T) = H_0(T) + q(1 - \sqrt{1 - R^2}), \tag{7}$$

and

$$\frac{dN_i}{dT} = K_{\mathrm{on}}^{(i)}(R)(1 - N_i) - K_{\mathrm{off}}N_i \qquad (i = 1, 2), \tag{8}$$

where the attachment rate constants in dimensionless variables are $K_{\mathrm{on}}^{(i)} = 1$ for $H \le (\frac{1}{2\beta})^{1/2} + \mathcal{L}_i$ and $K_{\mathrm{on}}^{(i)} = [2\beta(H - \mathcal{L}_i)^2]^{1/2} e^{-\beta(H-\mathcal{L}_i)^2}$ for $H > (\frac{1}{2\beta})^{1/2} + \mathcal{L}_i$. Three important dimensionless parameters appear in Eqs. (6)–(8): The parameter $q \equiv a/\ell_1$ (typical values $\approx 10^2 \gg 1$) characterizes the finite curvature of the particle, and the parameter $\beta \equiv (\frac{1}{2}\mathcal{K}_s\ell_1^2)/k_B\theta$ controls the attachment rate and is the thermal energy, while the parameter $\alpha \equiv 3\mu(n_{1,0}\mathcal{K}_s\ell_1)^{-1}(k_{\mathrm{on}}^{\max})$ contrasts the viscous time $\mu/(n_{1,0}\mathcal{K}_s\ell_1)$ and the chemical limiting binding time $(k_{\mathrm{on}}^{\max})^{-1}$. Of special relevance is the limit $\alpha \gg 1$, which corresponds to a system where the rate limiting step is the time for viscous drainage of the fluid from between the particle and the substrate. Finally, $\rho \equiv n_{2,0}/n_{1,0}$ is the ratio of the number density of total bonds of the two families and thus a measure of the contrast in grafting densities.

The sticking process is initiated with the base of the sphere at the rest height of the longest tethers chosen here to be family 1, i.e., $H(0) = 1$, with no initial bonds, so that $N_1(0) = N_2(0) = 0$. We start with a consideration of the case of a single family of irreversible bonds so that $N_2(R, T) = 0$ and $K_{\text{off}} = 0$. Then, solving the system (6)–(8) numerically shows that the kinetics of particle capture has two regimes—a rapid settling regime (I) followed by a much slower aging regime (II) as shown in Fig. 2(a). In the settling regime, bonds attach over a characteristic region and the colloid descends rapidly towards the surface. This phase terminates at a height when central tensile forces, which push the sphere away from the substrate, balance the dominant peripheral compressive forces over a region with vertical extent $\beta^{-(1/2)}$. A scaling estimate of this height gives $(1 - H_0^*) \sim \beta^{-(1/2)}$. The characteristic region of adhesion over which the initial binding occurs is $R^* \sim q^{-(1/2)}\beta^{-(1/4)}$ (Supplemental Material, Sect. II [19]). Within this region, all bonds are in their bound state. Outside this region, bonds attach very slowly—a larger fraction binding as time increases. The region of adhesion grows very slowly, as the bonds need to make very long excursions compared to their rest length to be able to stick to the particle, and the balance between the attractive forces due to slowly attaching bonds and viscous resistance to fluid drainage determines the settling speed (regime II). We find that the initial stages of regime II may be described analytically (Supplemental Material, Sect. II [19]). Past the initial rapid descent, the sphere begins to descend slowly with the sphere height decaying as

$$H_0 \approx H_0^* \exp(-t/\tau_{\text{aging}}), \quad \text{with} \quad \tau_{\text{aging}} \sim q\alpha\beta \tag{9}$$

setting the characteristic time scale of the aging phase. This scaling for the decay rate is valid so long as the radius of adhesion is less than $\sqrt{H_0/q}$. The ultimate dynamics once binders attach at $R \gg \sqrt{H_0/q}$ is, however, even slower than the above equation suggests (Supplemental Material, Sect. II [19]), and the sphere makes physical contact with the substrate only as $T \to \infty$ due to the divergence of the viscous drag term. In the final state, the binders exert a net positive force pushing the sphere towards the surface, and hence energy has to be expended in order to dislodge the sphere. This final bound state can be understood as the end result of a series of differential stages. At each stage of the descent, additional bonds must attach to the periphery (at increasingly larger R) and then draw the colloid closer to the substrate below until the elastic forces are in approximate balance with the adhesion radius attaining a certain value. The sphere waits (albeit, momentarily) and then executes the next stage once bonds attach again beyond the adhesion region established previously.

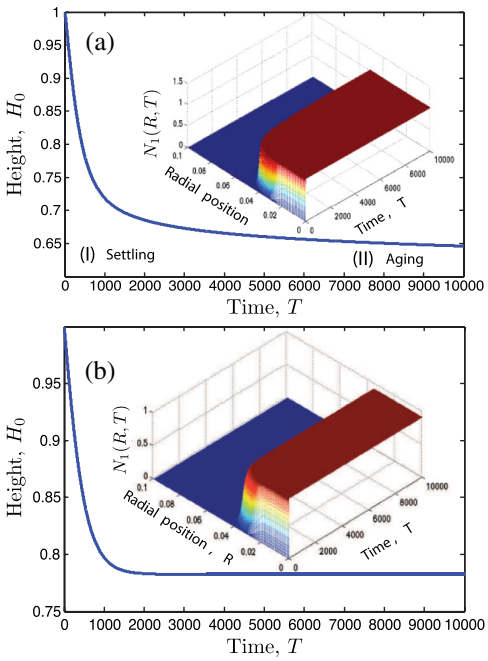

FIG. 2 (color online). The height of the particle, H_0, as a function of time T for a one-family binder system with $N_{2,0} = 0$, $\alpha = 100$, $\beta = 100$, $q = 500$, and $H_0(T = 0) = 1$. (a) $K_{\text{off}} = 0$: An initial steep descent to a critical height is followed by a slow aging process with H_{eq} decaying exponentially to 0. (b) $K_{\text{off}} \neq 0$: Unlike in (a), the region of adhesion is bounded and the particle settles to a nonzero equilibrium height. The insets show the evolution of attached bond density when there is no unbinding and where there is some unbinding.

The settling scenario changes quite dramatically if one allows for even a small detachment rate. In Fig. 2(b), we show that the tail of the bound tether distribution now has a cutoff at $H = H_{\text{cutoff}}$ determined by the detachment rate $K_{\text{on}}^{(1)} \approx e^{-\beta(H_{\text{cutoff}}-1)^2} = K_{\text{off}}$, thereby modifying the equilibrium height to a nonzero offset that is $O(\sqrt{|\ln K_{\text{off}}|})$ provided that $q \gg 1$. In the absence of any other influences, contact between the particle and substrate is avoided, and the particle settles down as a nonzero height.

Inclusion of additional families of tethers with different equilibrium height distributions leads to a series of punctuated regimes of adhesion. In each regime, the slow aging process at the previous level results in the colloid being brought into reach of the shorter families of tethers. Their binding results in the rapid motion of the colloid before slowing and a subsequent repeat of the same process. Figures 3(a)–3(c) display the effect of having a second family of bonds with $\ell_2 < \ell_1$ with the bonds attaching irreversibly. Four distinct regimes are seen—the first corresponds to the initial settling regime for the single family case; the second is the aging dynamics associated with the first family, drawing it towards the substrate slowly. When $H_0 \sim \ell_2 + 1/\sqrt{2\beta}$, a strong transition in the particle position is seen—evidenced by the knee in Fig. 3(a) at a time $T \approx T^*$. An increasing number of shorter bonds from the second family bind onto the particle, and

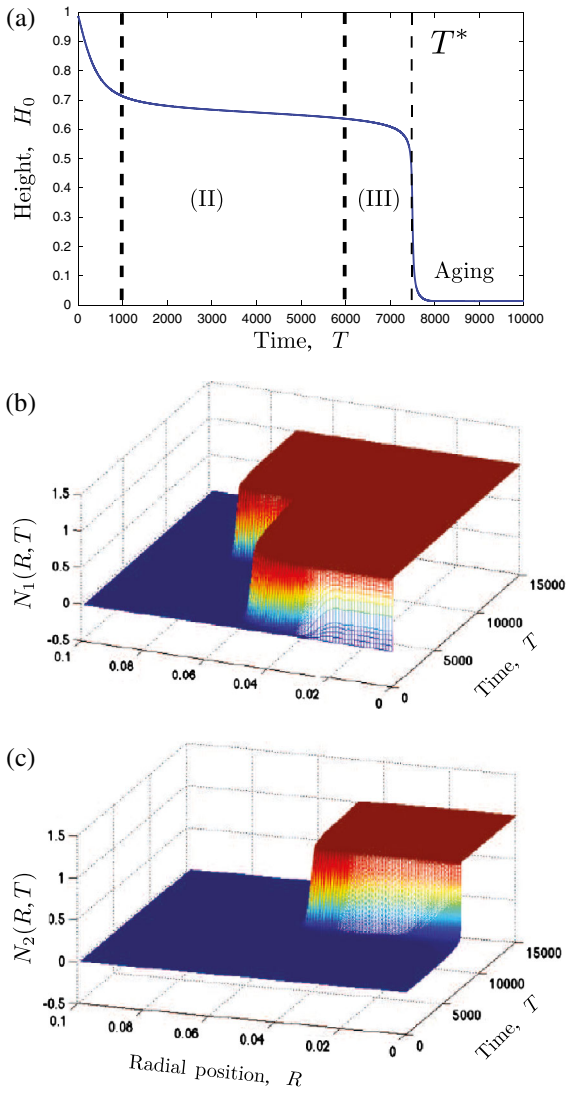

FIG. 3 (color online). Adhesion dynamics due to a two-family system for parameters $N_{2,0}/N_{1,0} = 100$, $K_{\rm off} = 0$, $\alpha = 100$, $\beta = 100$, $\mathcal{L}_2 = 0.25$, and $q = 500$. (a) Height H_0 versus time T. (b),(c) N_1 and N_2 as a function of radial distance from origin, R, and time T, respectively.

the exponentially slow decay transitions to a more rapid descent. An estimate of the time interval T^* may be obtained when the expression for the settling rate—Eq. (9)—is valid long enough for the particle to descend to a height $H \approx \mathcal{L}_2 + 1/\sqrt{\beta}$, when the second set of adhesive bonds start to bind. The time T^* is then given by (Supplemental Material, Sect. II [19])

$$T^* \sim q\alpha\beta \left| \ln \frac{\mathcal{L}_2 + 1/\sqrt{2\beta}}{H_0^*} \right|. \tag{10}$$

Our analysis has led to a simple picture for the kinetics of adhesion as limited by the dynamics of fluid drainage between the particle and the substrate. Our simple model for adhesive capture relates microscopic features such as

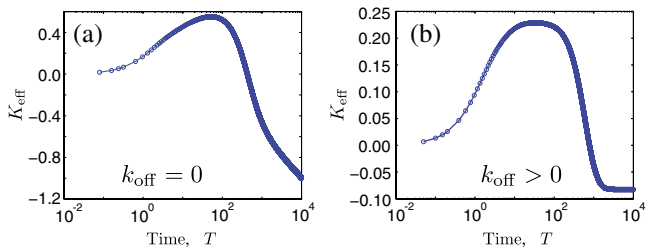

FIG. 4 (color online). The transverse linear elastic compliance $K_{\rm eff}$ due to the linear elasticity of attached binders for (a) $k_{\rm off} = 0$ and (b) $k_{\rm off} > 0$. As the sphere settles, the sign of the resultant elastic force changes. Parameter values are the same as in Fig. 2.

kinetics and elasticity of individual adhesive bonds to macroscopically measured settling rates and aging times. We observe punctuated motion of the particle towards the substrate, which is an outcome of rare binding events. Such a punctuated aging process has been recently observed and been hypothesized to reflect a small number of metastable minima accessible to the system during attachment [3] in agreement with our interpretation. Although the punctuated aging process investigated here is due to families of binders with distinct rest lengths, similar effects would follow if the tethers were nonlinearly elastic. Additional effects due to steric hindrance and hydrodynamic or electrostatics effects on tether motions may also alter the dynamics [12,13], but we expect the gross features of the process to be preserved nonetheless.

We conclude with a brief discussion of the elastic response of the adhesively bound particle that stores elastic energy in the bonds which are compressed at the point of closest approach and extended away from it. This nonuniformity should lead to a nontrivial transverse linear compliance of the adhered particle when the sphere is subject to small amplitude, high frequency transverse displacements (Supplemental Material, Sect. III [19]). As the particle ages, it is unstable to small transverse displacements, whence the effective linear elastic compliance of the system, $K_{\rm eff} \sim 2\pi \sum_i \int_0^a \mathcal{K}_s n_i(r,t)(\frac{h-\ell_i}{h}) r dr$, is seen to change sign and become negative as the sphere gets closer to the substrate, as shown in Fig. 4 for both the case when the binders may detach or not. The physical mechanism underlying this linear instability is that attached binders near the center line are compressed while those attached far away are extended, so that the particle can move sideways and eventually has a soft mode associated with movement in a circle around the energetic minimum due to a competition between tether shear and compression. Incorporation of higher order terms and allowing bonds to attach at an angle to the vertical regularize this behavior. A careful experimental test of our theory is an obvious next step.

Funding for this research was provided by NIH via Grant No. 1R21HL091331-02 and the MacArthur Foundation (L. M.).

*Present address: KITP and UCSB Physics, Santa Barbara, CA, USA.
†Corresponding author.
lm@seas.harvard.edu

[1] P. G. Wolynes and J. A. McCammon, Macromolecules **10**, 86 (1977).
[2] J. C. Crocker, Nature (London) **451**, 528 (2008).
[3] P. Sharma, S. Ghosh, and S. Bhattacharya, Nature Phys. **4**, 960 (2008); J. Chem. Phys. **133**, 144909 (2010); Appl. Phys. Lett. **97**, 104101 (2010).
[4] G. I. Bell, Science **200**, 618 (1978).
[5] D. Hammer and S. Apte, Biophys. J. **63**, 35 (1992).
[6] J. T. Groves, L. K. Mahal, and C. R. Bertozzi, Langmuir **17**, 5129 (2001).
[7] S. R. Hodges and O. E. Jensen, J. Fluid Mech. **460**, 381 (2002).
[8] S. W. Schneider, S. Nuschele, A. Wixforth, C. Gorzelanny, A. Alexander-Katz, R. R. Netz, and M. F. Schneider, Proc. Natl. Acad. Sci. U.S.A. **104**, 7899 (2007).
[9] R. D. Duffadar and J. M. Davis, J. Colloid Interface Sci. **326**, 18 (2008).
[10] M. Dembo, D. C. Torney, K. Saxman, and D. Hammer, Proc. R. Soc. B **234**, 55 (1988).
[11] U. Seifert, Phys. Rev. Lett. **84**, 2750 (2000).
[12] A. Gopinath and L. Mahadevan, Proc. R. Soc. A **467**, 1665 (2011).
[13] G. H. Fredrickson and P. Pincus, Langmuir **7**, 786 (1991).
[14] When this is no longer true, the array of binders in the fluid behaves like a poroelastic carpet [12], and our theory must be revisited.
[15] J. Happel and H. Brenner, *Low Reynolds Number Hydrodynamics* (Martinus Nijhoff, The Hague, 1983).
[16] H. A. Kramers, Physica (Utrecht) **7**, 284 (1940).
[17] D. Vella and L. Mahadevan, Langmuir **22**, 163 (2006).
[18] N. G. Van Kampen, *Stochastic Processes in Physics and Chemistry* (Elsevier, New York, 1981).
[19] See Supplemental Material at http://link.aps.org/supplemental/10.1103/PhysRevLett.108.226104 for additional theoretical details.